

Detection of X-ray Resonance Scattering in Active Stellar Coronae

Paola Testa^{1,2,3}, Jeremy J. Drake², Giovanni Peres³ and Edward E. DeLuca²

ABSTRACT

An analysis of Lyman series lines arising from hydrogen-like oxygen and neon ions in the coronae of the active RS CVn-type binaries II Peg and IM Peg, observed using the *Chandra* High Resolution Transmission Grating Spectrograph, shows significant decrements in the $\text{Ly}\alpha/\text{Ly}\beta$ ratios as compared with theoretical predictions and with the same ratios observed in similar active binaries. We interpret these decrements in terms of resonance scattering of line photons out of the line-of-sight; these observations present the first strong evidence for this effect in active stellar coronae. The net line photon loss implies a non-uniform and asymmetric surface distribution of emitting structures on these stars. Escape probability arguments, together with the observed line ratios and estimates of the emitting plasma density, imply typical line-of-sight sizes of the coronal structures that dominate the X-ray emission of 10^{10} cm at temperatures of 3×10^6 K and of 10^8 cm at 10^7 K. These sizes are an order of magnitude larger than predicted by simple quasi-static coronal loops models, but are still very small compared to the several 10^{11} cm radii of the underlying stars.

Subject headings: Radiative transfer — X-rays: stars — stars: coronae — stars: late type

1. Introduction

The Sun is the only star for which we can presently image coronal X-ray emission, and in order to understand how coronae on other stars might be structured we must resort to indirect means. One potentially powerful diagnostic of the characteristic size of X-ray

¹SAO Predoctoral Fellow

²Smithsonian Astrophysical Observatory, MS 3, 60 Garden Street, Cambridge, MA 02138, USA; jdrake@head.cfa.harvard.edu

³DSFA, Sezione di Astronomia, Università di Palermo Piazza del Parlamento 1, 90134 Palermo, Italy

emitting regions is line quenching through resonance scattering. The escape probability of a photon emitted by a resonance line in a low density homogeneous plasma is dependent on the line-of-sight path length through the plasma region. Provided the plasma density and the abundance fraction of the ion in question are known, in the regime where the plasma is only marginally thick the comparison of strong and weak lines subject to different scattering losses can yield an estimate of the typical emitting region path length.

Resonance scattering in the solar corona has been studied predominantly in the light of the strong ($gf = 2.66$) $2p^6\ ^1S_0 \rightarrow 2p^53d^1P_1$ resonance line of Fe XVII at 15.02 Å as compared to nearby weaker Fe XVII lines, though with controversial results concerning whether optical depth effects were seen or not (Phillips et al. 1996; Phillips et al. 1997; Schmelz et al. 1997; Saba et al. 1999). Studies of the same transition seen in different stars observed at high resolution ($\lambda/\Delta\lambda \sim 1000$) by *Chandra* have also recently been presented by Phillips et al. (2001) and Ness et al. (2003). Both stellar studies failed to find evidence for significant optical depth.

There are two problems with using the prominent Fe XVII soft X-ray complex for optical depth studies. Recently, it has been shown by Doron & Behar (2002) and Gu (2003) that the indirect processes of radiative recombination, dielectronic recombination, and resonance excitation involving the neighbouring charge states are important for understanding the relative strengths of Fe XVII–XX lines. Secondly, the coronae of active stars have been found to be Fe-poor by factors of up to 10 compared with a solar or local cosmic composition (e.g. reviews by Drake et al. 2003, Audard et al. 2003), reducing the sensitivity of Fe lines as optical depth indicators. Indeed, the spectral lines likely to exhibit the largest optical depths in the coronae of active stars are the Lyman α lines of hydrogen-like O and Ne—elements that are often seen to be enhanced relative to Fe (e.g. Drake et al. 2001, Audard et al. 2003).

In this *Letter*, we present an analysis of the Ly α to Ly β line strength ratios in the active binaries II Peg and IM Peg, and show that the Ly α lines of Ne and O are significantly quenched. We use inferred optical depths to make the first direct estimates of the dimensions of coronal structures in active stars.

2. Observations and Analysis

Observations and relevant characteristics of the program stars are summarised in Table 1. All spectra were obtained by the *Chandra* High Energy Transmission Grating (HETG) in conjunction with the Advanced CCD Imaging System spectroscopic detector (ACIS-S),

and were downloaded from the *Chandra* Data Archive¹. Spectra from multiple observations (IM Peg and AR Lac) were combined, and positive and negative orders were summed, keeping HEG and MEG spectra separate. The same observations of HR 1099, II Peg and AR lac are described in more detail by Drake et al. (2001), Huenemoerder et al. (2001) and Huenemoerder et al. (2003), respectively.

Resonance scattering of Ly α and Ly β photons can be diagnosed by comparison of the measured Ly α /Ly β ratio with respect to the theoretical ratio. Spectral line fluxes were measured using the FITLINES utility in the PINTofALE² IDL³ software package (Kashyap & Drake 2000). In the case of O VIII, the Ly β transition is blended with an Fe XVIII line ($2s^22p^5\ ^2P_{3/2} - 2s^22p^4(^3P)3s\ ^2P_{3/2}$, $\lambda = 16.004\ \text{\AA}$). We estimated its intensity by scaling the observed intensity of the neighbouring Fe XVIII $16.071\ \text{\AA}$ ($2s^22p^5\ ^2P_{3/2} - 2s^22p^4(^3P)3s\ ^4P_{5/2}$) transition, that shares the same upper level, by the ratio of their theoretical line strengths (0.76) as predicted by the APED database (Smith et al. 2001). Uncertainties involved in this deblending procedure are negligible for II Peg (whose Fe XVIII is weak) and similar to or less than Poisson errors for the other stars for, e.g., an error of $\sim 20\%$ in the theoretical Fe XVIII ratio. He-like resonance lines of Ne IX and O VII were also measured in order to derive a temperature estimate from the Ly α /He-like r ratio. Measured line fluxes and statistical errors are listed in Table 2.

Observed and theoretical O and Ne Ly α /Ly β ratios are compared in Figure 1. The observed ratios are shown at the temperatures at which observed H-like to He-like $2p$ - $1s$ line intensities matched their theoretical (APED) values (see Table 3). While it is an approximation to assume that the lines are formed at a single temperature, this is not critical because the temperature dependences of these Ly α /Ly β ratios are not steep for $T > 2$ MK. Both O and Ne H-like lines are formed at temperatures significantly lower than those at which the theoretical Ly α /Ly β ratios reach their asymptotic limits.

The observed Ly α /Ly β ratios are lower than the theoretical values for both the Ne X and the O VIII lines in the case of IM Peg, and for O VIII in II Peg. Huenemoerder et al. (2001) noticed similar discrepancies in II Peg but excluded optical depth effects on the grounds that this deviation was less than $\sim 2\sigma$ from the theoretical value; it appears, however, that this assessment was based on the high temperature asymptotic ratio of ~ 6.25 (in photon units). Our measured ratio for II Peg is instead more than 3σ lower than the expected ratio at the temperature of formation of the O VIII lines. In the case of IM Peg, the observed O VIII

¹<http://cxc.harvard.edu/cda>

²<http://hea-www.harvard.edu/PINTofALE/>

³Interactive Data Language, Research Systems Inc.

ratio lies $\sim 1.8\sigma$ below the theoretical value, while the Ne X ratio in both HEG and MEG, are $> 3\sigma$ lower. For comparison with IM Peg and II Peg, we also present similar results for AR Lac and HR 1099: these ratios instead do not show significant departure from the expected optically thin values.

Though uncertainties in the theoretical ratio are not included, these are not expected to exceed 10% based on good agreement with recent laboratory experiments (G. Brown, private communication; Beiersdorfer 2003). If we assume a 10% error in theoretical ratios, the Ne $\text{Ly}\alpha/\text{Ly}\beta$ of IM Peg still departs by 3σ for MEG ($\sim 1.7\sigma$ for HEG), while the O ratios lie 2.5σ for II Peg and 1.3σ for IM Peg below the theoretical curve. In Figure 1, we also plot the O VIII $\text{Ly}\alpha/\text{Ly}\beta$ ratios obtained from the line fluxes measured by Raassen et al. (2002) from *Chandra*/LETGS and *XMM-Newton*/RGS1 spectra of Procyon. In the Procyon spectrum Fe XVIII is not detected and these data provide further validation of the APED O VIII $\text{Ly}\alpha/\text{Ly}\beta$ ratio.

These quantitative results are reinforced by a visual comparison of spectra in Figure 2, in which the $\text{Ly}\alpha$ lines in II Peg and IM Peg are visibly weaker relative to $\text{Ly}\beta$ than those of AR Lac and HR 1099. There do not appear to be plausible explanations for the discrepant ratios other than by the quenching of $\text{Ly}\alpha$ relative to $\text{Ly}\beta$ through resonance scattering within the emitting plasma. Intervening photoelectric absorption could cause similar effects but H column densities of order a few 10^{21} cm^2 would be required—two or three orders of magnitude higher than inferred for these stars (Mewe et al. 1997; Mitrou et al. 1997).

2.1. Path Length Estimate

Our measured line ratios allow us to derive an effective optical depth τ , and a typical photon path length within the emitting plasma. We use the escape probability, $p(\tau)$, derived by Kastner & Kastner (1990), which for $\tau \lesssim 50$ can be approximated by (e.g. Kaastra & Mewe 1995)

$$p(\tau) \sim \frac{1}{1 + 0.43 \tau}. \quad (1)$$

This is the escape probability for line photons emitted at optical depths between 0 and τ , averaged over a Gaussian line profile due to thermal Doppler broadening, and it assumes that each scattered photon is completely lost from the line of sight. This probability is significantly larger than the $e^{-\tau}$ transmittance of the simple absorption case, since it assumes emission over the whole line of sight through the plasma. The line center optical depth, τ , can be

written (e.g., Acton 1978):

$$\tau = 1.16 \cdot 10^{-14} \cdot \frac{n_i}{n_{\text{el}}} A_Z \frac{n_{\text{H}}}{n_{\text{e}}} \lambda f \sqrt{\frac{M}{T}} n_{\text{e}} \ell \quad (2)$$

for ion fraction n_i/n_{el} (from Mazzotta et al. 1998), element abundance A_Z , oscillator strength f , temperature T , electron density n_{e} , atomic weight M , where $n_{\text{H}}/n_{\text{e}} \sim 0.85$, and ℓ is the total path length along the line of sight through the emitting plasma. In the above, neglect of non-thermal broadening should not be important: non-thermal velocities of, e.g., 50 km s^{-1} —similar to the thermal velocities for O and Ne at their characteristic temperatures of formation—would result in ℓ being underestimated by a factor of 1.4.

Electron densities were adopted from the survey of Testa et al. (2004; hereafter Paper I): for $\tau(\text{O VIII})$ we assumed the n_{e} derived from the O VII He-like triplet; the Ne IX triplet is strongly affected by blends with Fe lines and so for $\tau(\text{Ne X})$ we assumed the n_{e} derived from the Mg XI He-like triplet that forms at a similar temperature. In the case of IM Peg, the low signal in the O VII intercombination and forbidden lines precludes a firm density estimate; we therefore assumed a value of $2 \times 10^{10} \text{ cm}^{-3}$, which is typical of values obtained for all the measurable spectra of RS CVns in Paper I. The assumed n_{e} are listed in Table 3, while the adopted O and Ne abundances are listed in Table 4.

In order to derive an estimate of the path length, ℓ , we treated the fine structure components of Ly α (1: ${}^2P_{3/2} \rightarrow {}^2S_{1/2}$ at $\lambda = 18.9671 \text{ \AA}$ and 2: ${}^2P_{1/2} \rightarrow {}^2S_{1/2}$ at $\lambda = 18.9726 \text{ \AA}$) separately, since their splitting ($\Delta\lambda/\lambda \sim 0.0003$) is larger than the thermal width ($\sim \sqrt{k_B T/M}/c \sim 0.00013$). The observed and theoretical intensities, I_{obs} and I_{th} , are then related as follows:

$$I_{\text{Ly}\alpha \text{ obs}} = I_{1 \text{ obs}} + I_{2 \text{ obs}} = \frac{I_{1 \text{ th}}}{1 + 0.43\tau_1} + \frac{I_{2 \text{ th}}}{1 + 0.43\tau_2}. \quad (3)$$

Since for hydrogenic ions $f_2 = f_1/2 = 0.2776/2$ (e.g. Morton 2003), $I_{2 \text{ th}} = I_{1 \text{ th}}/2$, and $\tau_i \sim C(\ell) \cdot f_i$ (see Eq. 2), we obtain:

$$\frac{I_{\text{Ly}\alpha \text{ obs}}}{I_{\text{Ly}\alpha \text{ th}}} = \frac{1}{3} \left[\frac{2}{1 + 0.43C(\ell)f_1} + \frac{1}{1 + 0.43C(\ell)f_1/2} \right]. \quad (4)$$

For Ly β the splitting of the components is smaller than the thermal width and the escape probability for Ly β is given directly by Eq.1. The combined equation for $C(\ell)$ was then solved to obtain the path length.

The path length estimates, ℓ_{τ} , derived from the measurements are listed in Table 4. For comparison, we also list the stellar radii and loop lengths expected for a standard hydrostatic

loop model (e.g. Rosner et al. 1978, RTV hereafter), L_{RTV} , corresponding to the observed temperatures and densities.

3. Discussion and Conclusions

The discrepant O VIII and Ne X $\text{Ly}\alpha/\text{Ly}\beta$ ratios found here for II Peg and IM Peg represent the first clear evidence of resonant scattering in coronal X-ray emission lines. The photon path lengths inferred from the observed ratios (Table 4) are: (1) about two orders of magnitude different from each other, reflecting the differences in the plasma densities found in Paper I for the characteristic temperatures of formation of the O VIII and Ne X lines; (2) very small with respect to the stellar radius; (3) an order of magnitude larger than the loop lengths derived from RTV model scaling laws. In the ratio $\ell_{\tau}/L_{\text{RTV}}$ the n_e terms cancel, so that this conclusion is completely independent of plasma density measurements.

We note that the path lengths obtained from this type of analysis should be treated as lower limits because addition of $\text{Ly}\alpha$ photons by any optically thin emission or any scattering into the line-of-sight are not taken into account. In the case of a uniform spherically-symmetric arrangement of emitting structures over the stellar surface, scattering into and out of the line-of-sight would be expected to compensate one another. The detection of resonance scattering implicitly suggests a non-uniform coronal distribution.

That we find different optical depths in emitting regions on what are ostensibly similar active RS CVn-type binaries is puzzling. One possibility is that this is transient behaviour that might occur on all similarly active stars for a preferential arrangement of one or more coronal structures. We also note that, whereas both AR Lac and HR 1099 comprise two late-type stars of more similar type, II Peg and IM Peg have unseen companions of unknown spectral type, though how this arrangement might benefit larger coronal photon path lengths is not obvious.

We thank the referee, Jeffrey L. Linsky, for helpful comments that enabled us to improve the manuscript. PT was partially supported by *Chandra* grants GO1-20006X and GO1-2012X under the SAO Predoctoral Fellowship program. JJD was supported by NASA contract NAS8-39073 to the *Chandra X-ray Center*; EED was supported by NASA grant NAG5-10872. GP and PT were partially supported by MIUR and by ASI.

Table 1. Properties of Observed Stars and related HETG observations.

Source	Spectr.Type	d ⁽¹⁾ [pc]	R _* /R _⊙	P _{orb} ⁽²⁾ [ksec]	P _{rot} ⁽²⁾ [ksec]	L _X [HEG] ^a [erg/sec]	L _X [MEG] ^a [erg/sec]	F _X ^b [10 ⁵ erg/cm ² /sec]	Obs ID	t _{exp} [ksec]
II Peg	K2V/..	42	3.4/.. ⁽³⁾	580	580	1.56·10 ³¹	1.76·10 ³¹	250	1451	42.7
IM Peg	K2III-II/..	96.8	13/.. ⁽⁴⁾	2100	2100	2.75·10 ³¹	2.79·10 ³¹	27.1	2527	24.6
IM Peg						2.17·10 ³¹	2.30·10 ³¹	22.3	2528	24.8
IM Peg						1.86·10 ³¹	1.97·10 ³¹	19.2	2529	24.8
AR Lac	G2IV/K0IV	42	1.8/3.1 ⁽²⁾	170	170	5.21·10 ³⁰	5.60·10 ³⁰	284	6	32.1
AR Lac						5.61·10 ³⁰	6.30·10 ³⁰	319	9	32.2
HR 1099	G5IV/K1IV	29.0	1.3/3.9 ⁽²⁾	250	250	7.85·10 ³⁰	1.05·10 ³¹	1020	62538	94.7

^aHEG range: 1.5-15 Å; MEG range: 2-24 Å.

^bX-ray surface flux from L_X obtained from MEG spectra

Note. — References: ⁽¹⁾ SIMBAD database; ⁽²⁾ Strassmeier et al. 1993; ⁽³⁾ Berdyugina et al. 1998; ⁽⁴⁾ Berdyugina et al. 1999

Table 2. Line flux measurements and $Ly\alpha/Ly\beta$ ratios, with 1σ errors.

Source	grating	flux (10^{-6} photons cm^{-2} sec^{-1})							Photon Ratio	
		Ne X		Ne IX	O VIII		O VII	Fe XVIII	$Ly\alpha/Ly\beta$	
		$Ly\alpha$ 12.132Å	$Ly\beta$ 10.239Å	r 13.447Å	$Ly\alpha$ 18.967Å	$Ly\beta$ 16.006Å	r 21.602Å	16.071Å	Ne X	O VIII
II Peg	HEG	1364±70	160±28						8.5 ± 1.6	
	MEG	1217±28	178±8	365±21	2050±70	419±26	250±50	77±16	6.8 ± 0.3	5.6 ± 0.5
IM Peg	HEG	410±30	80±20						5.1 ± 0.9	
	MEG	385±13	71±2	77±11	530±40	145±22	52±25	55±13	5.4 ± 0.4	5.0 ± 1.2
AR Lac	HEG	727±30	106±11						6.8 ± 0.8	
	MEG	632±16	94±5	107±14	820±40	175±15	156±44	121±14	6.7 ± 0.4	9.9 ± 1.9
HR 1099	HEG	2180±40	288±13						7.6 ± 0.4	
	MEG	1705±21	222±6	571±16	2860±60	549±19	400±40	225±14	7.7 ± 0.2	7.6 ± 0.5

Table 3. Plasma densities and Temperatures.

			II Peg	IM Peg	AR Lac	HR 1099
n_e ^a	Mg XI	(10^{12}cm^{-3})	$5.6_{-2.5}^{+0.6}$	$3.2_{-1.4}^{+2.5}$	< 1.8	$1.8_{-0.5}^{+0.6}$
n_e ^a	O VII	(10^{10}cm^{-3})	$3.2_{-1.4}^{+6.8}$	-	-	$1.0_{-0.8}^{+2.2}$
T ^b	Ne	(MK)	6.7-7.3	7.8-8.8	8.1-9.6	6.0-6.4
T ^b	O	(MK)	4.7-5.5	4.5-7	4-5	4.7-5

^aFrom He-like triplet diagnostics (Paper I).

^bFrom $\text{Ly}\alpha/\text{r}$ ratio diagnostics.

Table 4. Path length derived from measured $\text{Ly}\alpha/\text{Ly}\beta$.

Source	Ion	Element ^a Abundance	ℓ_τ [cm]	L_{RTV} ^b [cm]	ℓ_τ/R_\star ^c
II Peg	O VIII	8.97 ^d	$9.5 \cdot 10^9$	$1 \cdot 10^9$	0.04
IM Peg	O VIII	9.37 ^e	$1.7 \cdot 10^{10}$	$2.2 \cdot 10^9$	0.019
	Ne X [HEG]	8.86 ^e	$1.6 \cdot 10^8$	$2.8 \cdot 10^7$	0.0002
	Ne X [MEG]	...	$2.2 \cdot 10^8$	$2.8 \cdot 10^7$	0.00018

^aExpressed on the usual spectroscopic logarithmic scale where $X/H = \log(n(X)/n(H)) + 12$, and $n(X)$ is the number density of the element X.

^bLoop length from RTV scaling laws: $L_{\text{RTV}} \sim T^2 / [(1.4 \cdot 10^3)^3 \cdot 2n_e k_B]$

^cPath length as fraction of the stellar radius

^dFrom Huenemoerder et al. (2001)

^eScaled from Huenemoerder et al. (2001) II Peg values by the ratio of II Peg to IM Peg photospheric metallicities, $[\text{Fe}/\text{H}]_{\text{II}} = -0.4$ and $[\text{Fe}/\text{H}]_{\text{IM}} = 0.0$, derived by Berdyugina et al. (1998,1999, respectively)

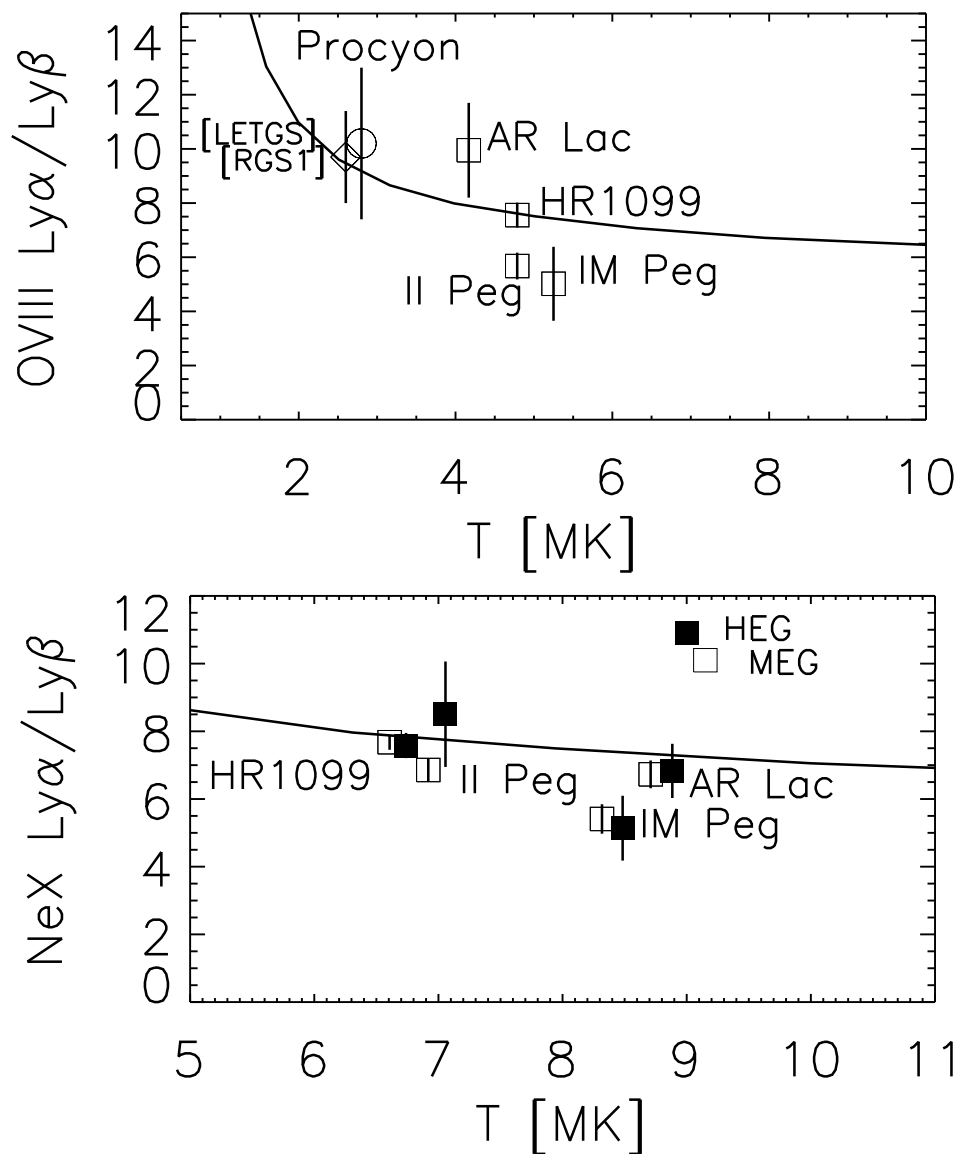


Fig. 1.— O VIII (*top*) and Ne X (*bottom*) Ly α /Ly β ratios for the analyzed sources vs. the temperature derived from the Ly α /He-like r diagnostics. The solid curve is the theoretical ratio from the APED database. For the Ne X we show the results from both the HEG (filled symbols) and the MEG (empty symbols) measurements; the HEG ratios are shifted by +5% on the T axis in order to distinguish the error bars corresponding to HEG and MEG measurements for the same source.

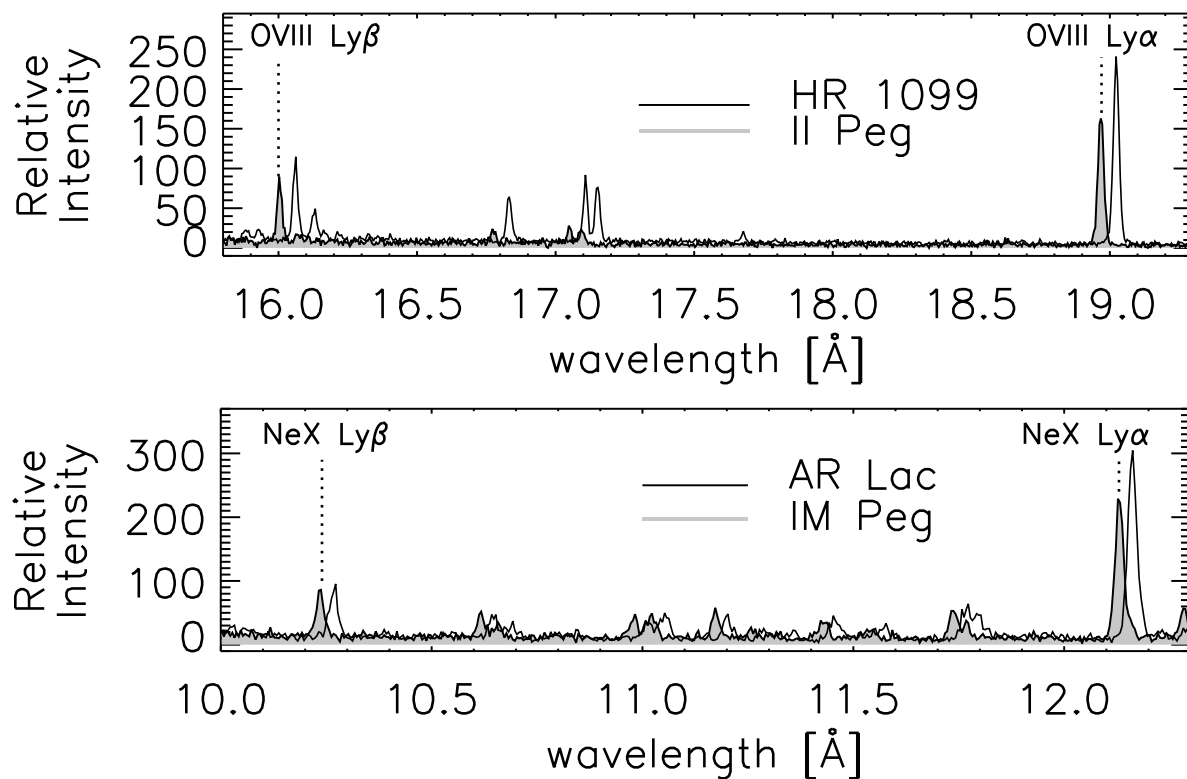


Fig. 2.— Comparison of the spectra for sources showing optical depth effects and sources appearing effectively optically thin. *Top* – O VIII Ly α, β spectral region for II Peg (filled profile) and HR 1099 (shifted in λ by $+0.06\text{\AA}$ for better readability). Spectra are normalised such that they have the same *unblended* Ly β line strength, i.e. after correction for the Fe XVIII line flux (see text). The different strengths of the Fe line complex near 17 \AA reflects primarily a different Fe/O abundance ratio in the two stars (Drake et al. 2001, Huenemoerder et al. 2001). *Bottom* – Ne X Ly α, β spectral region for IM Peg (filled spectrum) and AR Lac (shifted in λ by $+0.03\text{\AA}$ for better readability). Spectra are again normalized to the observed intensities of the Ly β line.

REFERENCES

- Acton, L.W. 1978, ApJ, 225, 1069
- Audard, M., Güdel, M., Sres, A., Raassen, A.J.J. & Mewe, R. 2003, A&A, 398, 1137
- Beiersdorfer, P. 2003, ARA&A, 41, 343
- Berdyugina, S.V., Jankov, S., Ilyin, I., Tuominen, I., Fekel, F.C. 1998, A&A, 334, 863
- Berdyugina, S.V., Ilyin, I., Tuominen, I. 1999, A&A, 347, 932
- Doron, R. & Behar, E. 2002, ApJ, 574, 518
- Drake, J.J. 2003, Advances in Space Research, 32, 945
- Drake, J.J., Brickhouse, N.S., Kashyap, V., Laming, J.M., Huenemoerder, D.P., Smith, R., Wargelin, B.J. 2001, ApJ, 548, L81
- Gu, M.F. 2003, ApJ, 593, 1249
- Huenemoerder, D.P., Canizares, C.R., Schulz, N.S. 2001, ApJ, 559, 1135
- Huenemoerder, D.P., Canizares, C.R., Drake, J.J., Sanz-Forcada, J. 2003, ApJ, 595, 1131
- Kaastra, J.S. & Mewe, R. 1995, A&A, 302, L13
- Kastner, S.O. & Kastner, R.E. 1990, JQSRT, 44, 275
- Kashyap, V. & Drake, J.J. 2000, Bull. Astron. Soc. India, 28, 475
- Mazzotta, P., Mazzitelli, G., Colafrancesco, S. & Vittorio, N. 1998, A&AS, 133, 403
- Mewe, R., Kaastra, J.S., van den Oord, G.H.J., Vink, J., Tawara, Y. 1997, A&A, 320, 147
- Mitrou, C.K., Mathioudakis, M., Doyle, J.G. & Antonopoulou, E. 1997, A&A, 317, 776
- Morton, D.C. 2003, ApJS, 149, 205
- Ness, J.-U., Schmitt, J.H.M.M., Audard, M., Güdel, M., Mewe, R. 2003, A&A, 407, 347
- Phillips, K.J.H., Mathioudakis, M., Huenemoerder, D.P., Williams, D.R., Phillips, M.E., Keenan, F.P. 2001, MNRAS, 325, 1500
- Phillips, K.J.H., Greer, C.J., Bathia, A.K., Coffey, I.H., Barnsley, R. & Keenan, F.P. 1997, A&A, 324, 381

- Phillips, K.J.H., Greer, C.J., Bathia, A.K. & Keenan, F.P. 1996, *ApJ*, 469, L57
- Raassen, A.J.J. et al. 2002, *A&A*, 389, 228
- Rosner, R., Tucker, W.H. & Vaiana, G.S. 1978, *ApJ*, 220, 643
- Saba, J.L.R., Schmelz, J.T., Bathia, A.K. & Strong, K.T. 1999, *ApJ*, 510, 1064
- Schmelz, J.T., Saba, J.L.R., Chauvin, J.C. & Strong, K.T. 1997, *ApJ*, 477, 509
- Smith, R.K., Brickhouse, N.S., Liedahl, D.A. & Raymond, J.C. 2001, *ApJ*, 556, L91
- Strassmeier, K.G., Hall, D.S., Fekel, F.C. & Scheck, M. 1993, *A&AS*, 100, 173
- Testa, P., Drake, J.J. & Peres, G. 2004, *ApJ*, in press